Lecture 5

Thermohaline Variability

Paola Cessi

1 Stochastic Forcing

The 2-box model analyzed in the prvious section (as well as Stommel's box-model) is governed by a deterministic equation, i.e. the time evolution of the salinity difference, σ, is completely determined by the model equation given an initial condition. Moreover, the system always reach one of two possible stable steady states. However, variability can be forced by a time-dependent forcing.

Now, let us consider a case where the salt flux, γ, has a component, γ', that is random in time, $\gamma = \bar{\gamma} + \gamma'(t)$. With the noise, σ is no longer a deterministic variable, but becomes a random variable. In this case, σ can be written as $\sigma = \bar{\sigma} + \sigma'(t)$.

Here, we consider two cases. For a weak agitation, or in a short time scale, the system oscillates near the stable steady states (See Figure 1). For a large agitation, it will shift from one stable point to another. In this section, we describe the behavior of the 2-box system using stochastic methods.

2 Rattle near stable points

For weak agitation, the system rattles almost linearly around each equilibrium. Assuming that the perturbation is small, we linearize the model equation around a stable solution, say $\bar{\sigma} = \sigma_c$. The time-dependendent perturbation satisfies

$$\frac{\partial \sigma'}{\partial t} = -\frac{\partial^2 V}{\partial \sigma^2}(\sigma_c)\sigma' + \gamma' \tag{1}$$

We use Fourier transforms to solve for the spectrum of σ'. The Fourier transform, $\tilde{\sigma}(\omega)$, of $\sigma'(t)$ is defined as:

$$\tilde{\sigma}(\omega) \equiv \frac{1}{2\pi}\int_{-\infty}^{\infty} \sigma'(t)\exp(-i\omega t)\,dt \tag{2}$$

$$\sigma'(t) = \int_{-\infty}^{\infty} \tilde{\sigma}\exp(i\omega t)\,d\omega \tag{3}$$

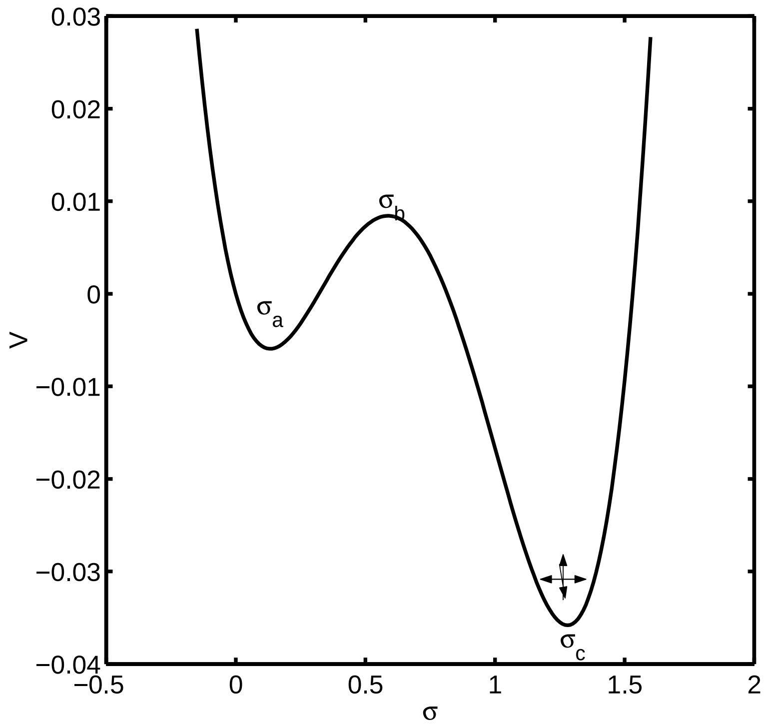

Figure 1: *Rattle near stable points:* Potential V is a function of σ. For weak noise, the system rattles around the steady states, σ_a, and σ_c.

And similarly, the Fourier transform pair of $\gamma'(t)$ is:

$$\tilde{\gamma}(\omega) \equiv \frac{1}{2\pi}\int_{-\infty}^{\infty} \gamma'(t)\exp(-i\omega t)\,dt \tag{4}$$

$$\gamma'(t) = \int_{-\infty}^{\infty} \tilde{\gamma}\exp(i\omega t)\,d\omega \tag{5}$$

Applying these relationship to (1), we obtain,

$$\tilde{\sigma} = \frac{\tilde{\gamma}}{V_{\sigma\sigma} + i\omega} \tag{6}$$

$\gamma'(t)$ is the stochastic noise, and is randomly picked at every timestep, dt, from a gaussian distribution with zero mean and variance ξ^2. The auto correlation of γ' is,

$$< \gamma'(t)\gamma'(t+\tau) > \approx \delta(\tau)dt\,\xi^2. \tag{7}$$

where $\delta(\tau)$ denotes a delta function in τ. The Fourier transform of a delta function is a constant, therefore, the spectrum (given by the ensemble average of the Fourier transform of the auto correlation function) $< |\tilde{\gamma}|^2 >$ is constant for all ω. Thus the spectrum of σ can be calculated by taking the product of (6) with its own complex conjugate and ensamble averaging to obtain:

$$< \tilde{\sigma}\tilde{\sigma^*} > = \frac{< \tilde{\gamma}\tilde{\gamma^*} >}{V_{\sigma\sigma}(\sigma_c)^2 + \omega^2} = \frac{dt\,\xi^2}{V_{\sigma\sigma}(\sigma_c)^2 + \omega^2}. \tag{8}$$

This spectrum is red since it decreases with increasing frequency, starting at a frequency of the order of the linear damping term.

3 Jumps between equilibria

On longer time scales or with larger variance of the noise, jumps between σ_a and σ_c can occur occasionally. To study the stochastic behavior of the model with the noise-induced jumps between equilibria, we go back to the nonlinear model equation with the noise term.

$$\dot{\sigma} = -\frac{\partial V(\sigma)}{\partial \sigma} + \gamma'(t). \tag{9}$$

The probability distribution function (hereafter, PDF), $\phi(\sigma, t)$, describes the probability of finding a particular value for σ at time t. The Fokker-Plank Equation (hereafter, FPE) describes the time evolution of the PDE of the stocastically forced system *[Gardiner 1990]*. The FPE of the 2-box model is,

$$\frac{\partial \phi}{\partial t} = (V_\sigma \phi)_\sigma + D\phi_{\sigma\sigma} \tag{10}$$

where $D \equiv \frac{\xi^2}{2}\,dt$. Taking the right hand side of the FPE to zero we obtain the steady state solution, ϕ_s, which is the probability of finding a state with a particular value of σ when time goes to infinity. The steady distribution is given by

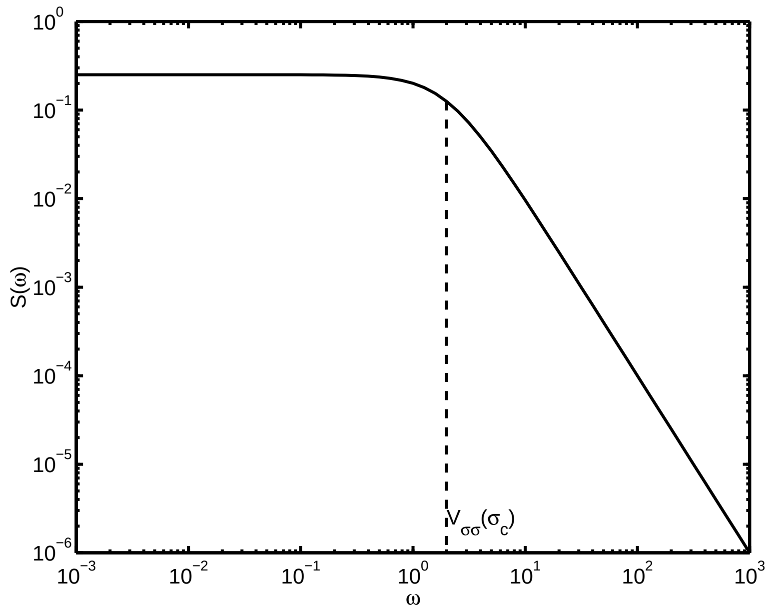

Figure 2: *Power spectrum of small perturbation around stable points*

$$\phi_s(\sigma) = N \exp(\frac{-V(\sigma)}{D}). \tag{11}$$

where N is a normalization constant which is determined by the constraint $\int_{-\infty}^{\infty} \phi_s \, d\sigma = 1$. Figure 3 shows an example of stationary distribution, ϕ_s, as a function of σ.

4 Average transit times

In this section, we calculate the average time for the system to shift from one stable equilibrium to another. First, let us calculate the probability, N_{ac}, of finding $\sigma_a \leq \sigma \leq \sigma_c$ at time t.

$$N_{ac} = \int_{\sigma_a}^{\sigma_c} \phi(x,t) \, dx \tag{12}$$

The probability N_{ac} can also be viewed as the probability that the time, τ, to exit the interval $[a,c]$, exceeds t. Indeed, finding σ in the range $[\sigma_a, \sigma_c]$ at time t implies that σ must leave the region after the time t. We define $q(\tau)$ as the PDF for the exit time, τ, from the region $[\sigma_a, \sigma_c]$.

$$N_{ac} = \int_{t}^{\infty} q(\tau) \, d\tau \tag{13}$$

Then, the average exit time is given as the first moment of the PDF, $q(t)$. Denoting with $T_{a\to c}$ the average time for σ to escape from the region $[\sigma_a, \sigma_c]$, we find:

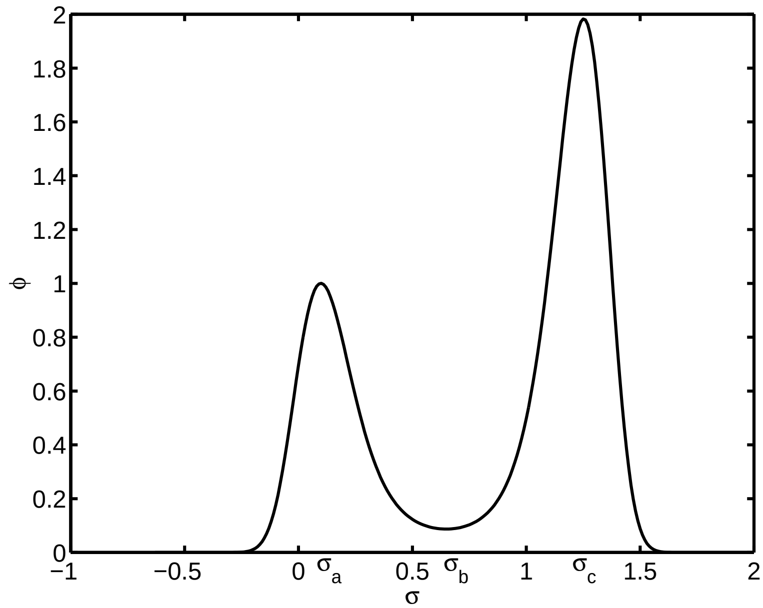

Figure 3: *Steady state of the PDF :* $\phi_s(\sigma)$

$$\begin{aligned} T_{a\to c} &= \int_0^\infty tq(t)\,dt \\ &= -\int_0^\infty t\frac{dN_{ac}}{dt}\,dt \\ &= \int_0^\infty N_{ac}\,dt. \end{aligned} \tag{14}$$

To find $T_{a\to c}$ we integrate the FPE with boundary conditions in time and space. The mean escape time from σ_c to σ_a, denoted with $T_{c\to a}$ can be also find using a similar procedure. The boundary conditions will specify the direction of the shift between equilibria.

Here, consider a case where σ moves from σ_a to σ_c. We assume that at $t = 0$, the model state, σ, is at σ_a, so that the PDF is a delta function. We also assume that as time goes infinity, the PDF goes to zero. Defining the time-integrated PDF, $\bar{\phi} \equiv \int_0^\infty \phi(\sigma, t)\,dt$ and integrating (10) in time from 0 to ∞ we find

$$-\delta(\sigma - \sigma_a) = (V_\sigma \bar{\phi})_\sigma + D\bar{\phi}_{\sigma\sigma}. \tag{15}$$

We also assume that $\bar{\phi} \to 0$ as $\sigma \to -\infty$ because σ moves from σ_a to σ_c, implying that once the particle has moved to σ_c, it should not return to the original location. This condition gives $\bar{\phi}(\sigma_c) = 0$. With these boundary conditions, one can solve equation (15), and obtain $T_{a\to c}$.

$$
\begin{aligned}
T_{a\to c} &= \frac{1}{D}\int_{\sigma_a}^{\sigma_c}\frac{dx}{\phi_s(x)}\int_{-\infty}^{x}\phi_s(y)\,dy \\
&\approx \frac{1}{D}\int_{\sigma_a}^{\sigma_c}\frac{dx}{\phi_s}\int_{-\infty}^{\sigma_b}\phi_s\,dy
\end{aligned} \tag{16}
$$

We calculate $T_{c\to a}$ using the same equation with different boundary conditions. In this case, the model state, σ is initially concentrated at σ_c and the PDF is delta function there. We assume that $\bar{\phi} \to 0$ as $\sigma \to \infty$ because σ moves from σ_c to σ_a (with $\sigma_a < \sigma_c$ as in figure 1). Also we set $\bar{\phi}(\sigma_a) = 0$, assuming that once particles arrive at σ_a they never come back. With these boundary conditions, we solve the equation (15), and obtain $T_{c\to a}$.

$$
T_{c\to a} \approx \frac{1}{D}\int_{\sigma_a}^{\sigma_c}\frac{dx}{\phi_s}\int_{\sigma_b}^{\infty}\phi_s\,dy \tag{17}
$$

5 Random Telegraph Process

On long timescales we can assume that the system simply jumps between the two equilibria. We ignore the rattle around each equilibrium and only allow σ to be in one equilibrium or another. In this case, we can approximate the system with a Random Telegraph Process : σ is in σ_a with probability $\frac{N_a}{N}$ or in σ_b with probability $\frac{N_b}{N}$. The sum of $\frac{N_a}{N}$ and $\frac{N_b}{N}$ is unity. We can now use the average escape times $T_{c\to a}$ and $T_{a\to c}$ to estimate the rates of transitions between equilibria. Specifically we have

$$
\dot{N}_a = -\omega_a N_a + \omega_c N_c \tag{18}
$$
$$
\dot{N}_c = -\omega_c N_c + \omega_a N_a \tag{19}
$$

where $\omega_a = T_{a\to c}^{-1}$ and $\omega_c = T_{c\to a}^{-1}$. Steady solutions are found equating the right hand sides to zero, so that

$$
N_a = N\frac{\omega_c}{\omega_a+\omega_c} \tag{20}
$$
$$
N_c = N\frac{\omega_a}{\omega_a+\omega_c} \tag{21}
$$

We can compute the low frequency spectrum by taking the Fourier Transform of the auto-correlation function. First, we define the auto-correlation function of the Random Telegraph process.

$$
\mathcal{C}(\tau) =< \sigma'(t)\sigma'(t+\tau) > \tag{22}
$$

where $\sigma' = \sigma - < \sigma >$. The average value for σ is $< \sigma >= \frac{1}{N}\sum_1^N \sigma = \sigma_a\frac{N_a}{N} + \sigma_c\frac{N_c}{N}$. We need the time-dependent equation for $\mathcal{C}(t)$. First, let us consider the equilibrium value at $\tau = 0$,

$$\mathcal{C}(0) = \frac{1}{N}\sum_{1}^{N}\sigma'^2 \tag{23}$$
$$= \frac{N_a}{N}{\sigma'_a}^2 + \frac{N_c}{N}{\sigma'_c}^2 \tag{24}$$
$$= \frac{N_a N_c}{N^2}(\sigma_a - \sigma_c)^2 \tag{25}$$
$$= \frac{(\sigma_a - \sigma_c)^2\omega_a\omega_c}{(\omega_a + \omega_c)^2} \tag{26}$$

Next we consider the state of the system at time, $0 + dt$. We can calculate the autocorrelation, $\mathcal{C}(dt)$, by counting the expected number of jumps between the two states. During the time period, dt, the switch $\sigma_a \rightarrow \sigma_c$ occurs with a probability of $\frac{N_a}{N}\omega_a\, dt$. Similarly, the switch $\sigma_c \rightarrow \sigma_a$ occurs with a probability of $\frac{N_a}{N}\omega_c\, dt$.

We can count all the possible states of the system at time, $0+dt$. First, we can estimate the number of states where σ is at σ_a during the interval $[0, dt]$. The number of this particular state is $N_a(1 - \omega_a\, dt)$. Secondly, we can estimate the number of states where σ is at σ_c during $[0, dt]$. The number of this particular state is $N_c(1 - \omega_c\, dt)$. Finally, we can estimate the number of states in the transition between the equilibrium. The number of this particular state is $(N_a\omega_a + N_c\omega_c)\, dt$. Taking these together, we find

$$\mathcal{C}(dt) = \sum_{1}^{N}\sigma'(dt)\sigma'(0) \tag{27}$$
$$= \underbrace{\frac{N_a}{N}(1 - \omega_a dt){\sigma'_a}^2}_{\sigma_a \text{ at } 0 \text{ and } dt} + \underbrace{\frac{N_c}{N}(1 - \omega_c dt){\sigma'_c}^2}_{\sigma_c \text{ at } 0 \text{ and } dt} + \underbrace{(\frac{N_a}{N}\omega_a + \frac{N_c}{N}\omega_c)dt\sigma'_a\sigma'_c}_{\text{in transit}} \tag{28}$$

We can now form the differential equation for $\mathcal{C}$ at time, $t = 0$.

$$\frac{\partial \mathcal{C}}{\partial t}|_{\tau=0} = -\frac{1}{N}(\omega_a + \omega_c)(N_a{\sigma'_a}^2 + N_c{\sigma'_c}^2) \tag{29}$$
$$= -(\omega_a + \omega_c)\mathcal{C}(0) \tag{30}$$

The solution of this equation is $\mathcal{C}(\tau) = \mathcal{C}(0)e^{-(\omega_a+\omega_c)\tau}$, with $\mathcal{C}(0)$ given by (28).

Thus, the low-frequency end of spectrum for the box-model subject to noise is given by:

$$S(\omega) = \mathcal{C}(0)^2\frac{2(\omega_a + \omega_c)}{(\omega_a + \omega_c)^2 + \omega^2} \tag{31}$$

Given the dependence of the espace times on the noise variance, the amplitude of the spectrum increases as the noise variance decreases.

$$S(0) = \frac{2(\sigma_a - \sigma_c)^2\omega_a\omega_c}{(\omega_a + \omega_c)^3} \tag{32}$$
$$\propto \exp(A\xi^{-2}) \tag{33}$$

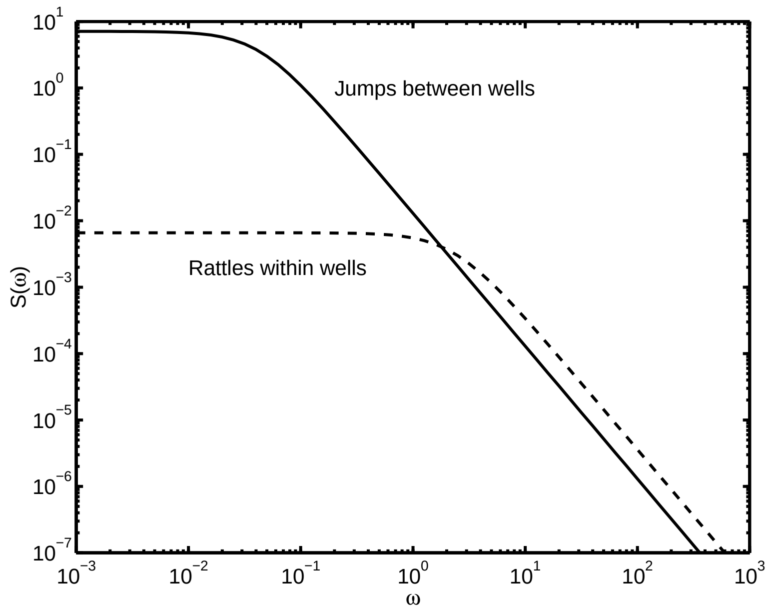

Figure 4: *The comparison of the short-time timescale and the long-timescale power spectrum*

Figure 4 compares the low-frequency and the high-frequency approximations. Note that the short-timescale spectrum represents the rattling around the stationary points, and saturates at higher frequency. The long-timescale spectrum approximates the jumps between the stationary points. Neither of the spectra show a peak because the associated deterministic system has only fixed points.

6 The Howard-Malkus-Welander loop

The next conceptual model that we will consider is the Howard-Malkus-Welander loop. A circular ring of fluid with temperature T and salinity S flows with angular velocity $\omega = \dot{\phi}$, with ϕ the angle to the vertical. The ring is immersed in a bath at constant temperature T_E and salinity S_E (see Fig. 5). The outer radius of the ring is r, the inner radius is a and g is gravity. For a thin loop with $(r - a) \ll a$, the fluid can be assumed to be well mixed in the radial direction, so that all variables become independent of r. In this case, the angular velocity satisfies the following equation

$$\dot{\omega} = -\frac{p_\phi}{\rho_0 a^2} - \frac{\rho g \hat{k} \cdot \hat{\phi}}{\rho_0 a} - \Gamma\omega. \tag{34}$$

Γ is the friction coefficient, $\hat{k}$ the unit vector in the vertical direction and $\hat{\phi}$ the unit vector in the tangential direction. Again we assume a linear equation of state, so that $\rho\hat{k} \cdot \hat{\phi} = \rho_0(\beta S - \alpha T)\sin\phi$.

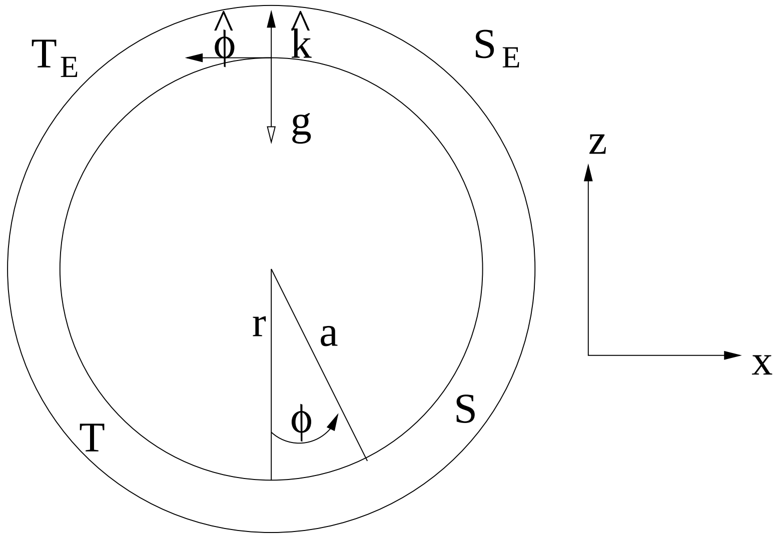

Figure 5: *Sketch of the Howard-Malkus-Welander loop.*

Equation (34) can be integrated around the loop to eliminate p and this yields

$$2\pi a\dot{\omega} = g\int_0^{2\pi} d\phi\,(\alpha T - \beta S)\sin\phi - 2\pi a\Gamma\omega \tag{35}$$

where we have used that, for a two-dimensional incompressible fluid, the angular velocity cannot depend on ϕ, if $\omega_r = 0$.

The temperature and salinity are determined through:

$$\begin{aligned}\dot{T} + \omega T_\phi &= r(T_E - T),\\ \dot{S} + \omega S_\phi &= r_s(S_E - S).\end{aligned}$$

where r and r_S are the diffusion rates of temperature and salinity, respectively. With antisymmetric forcing $(T_E, S_E) = (T_0, S_0)\sin\phi$ (heating and salting on the right side of the loop, cooling and freshening on the left side), we decompose temperature and salinity into a symmetric part and a antisymmetric part

$$T = T_1\cos\phi + T_2\sin\phi,\quad S = S_1\cos\phi + S_2\sin\phi.$$

Substitution of these relations in equation (36) yields

$$\begin{aligned}\dot{T}_1 + \omega T_2 = -rT_1, &\qquad \dot{T}_2 - \omega T_1 = r(T_0 - T_2),\\ \dot{S}_1 + \omega S_2 = -r_s S_1, &\qquad \dot{S}_2 - \omega S_1 = r_s(S_0 - S_2).\end{aligned}$$

For long time scales inertia will be much smaller than friction, $\dot{\omega} \ll \Gamma\omega$ and it follows directly from equation (35) that ω then satisfies

$$\omega = \frac{g}{2\Gamma a}(\alpha T_2 - \beta S_2). \tag{36}$$

In the limit where the relaxation rate of temperature is much greater than the relaxation rate of salinity, i.e. $r \gg r_s$, the temperature is clamped to the forcing, so that $T_1 \approx 0$, $T_2 \approx T_0$. The salinity evolves on a slower time-scale according to:

$$\begin{aligned}
\dot{S}_1 + \frac{g}{2\Gamma a}(\alpha T_0 - \beta S_2)S_2 &= -r_s S_1, \\
\dot{S}_2 - \frac{g}{2\Gamma a}(\alpha T_0 - \beta S_2)S_1 &= r_s(S_0 - S_2).
\end{aligned}$$

We introduce new variables $y_{1,2} = \frac{\beta S_{1,2}}{\alpha T_E}$ and $\hat{t} = \frac{g\alpha T_E}{2\Gamma a}t$, so that

$$\dot{y}_1 + (1 - y_2)y_2 = -\delta y_1 \tag{37}$$

$$\dot{y}_2 - (1 - y_2)y_1 = \delta(y_0 - y_2) \tag{38}$$

where a dot indicates now differentiation with respect to $\hat{t}$ with $\delta = \frac{2r_s\Gamma a}{g\alpha T_E}$.

The limit of a fixed salinity flux is given by $\delta \to 0$ with $\delta y_0 \equiv F$ finite. In this limit there is only one fixed point (the others are at ∞), given by

$$y_1 = -F, \quad y_2 = 0.$$

We can look at its linear stability by setting

$$y_1 = -F + \epsilon_1(t), \quad y_2 = \epsilon_2(t).$$

Neglecting $O(\epsilon^2)$ terms we find:

$$\dot{\epsilon}_1 + \epsilon_2 = 0, \quad \dot{\epsilon}_2 - \epsilon_1 - F\epsilon_2 = 0$$

These are the equations for an oscillator with damping $-F$:

$$\ddot{\epsilon}_2 + \epsilon_2 - F\dot{\epsilon}_2 = 0.$$

There is linear growth when $F > 0$, i.e. when the forcing is warm-salty and cold-fresh. When $F < 0$, the oscillations are damped out. Oscillations can only occur if the temperature and salinity forcing are opposing each other. Similarly, the Stommel 2-box model only admits multiple equilibria when there is competition between thermal and haline forcings.

The physical mechanism of the oscillation can be described as follows. As the fluid on the left flows downwards, it slows down due to the freshening. At the bottom it is now lighter and thus rises more rapidly on the right. Thus, it acquires less salt going up than it lost going down and at the next cycle it slows down even further. This leads to a growing alternation of slowing on the left and speeding on the right while going around the loop.

This oscillation occurs through a Hopf bifurcation at a certain value of the flux F, as illustrated in Figure 7: as the parameter F passes a certain value (in this case 0), the steady solution becomes oscillatory.

The period of this oscillation, $2\pi/\omega$, is the advection time around the loop and set by the thermally driven flow (see equation (36). For the North Atlantic, a similar advection time can be defined, which is about 100 years.

It is left to the reader to show that without salinity, but for general forcing, the steady state transport vanishes as $r \to 0$ when there is heating from above.

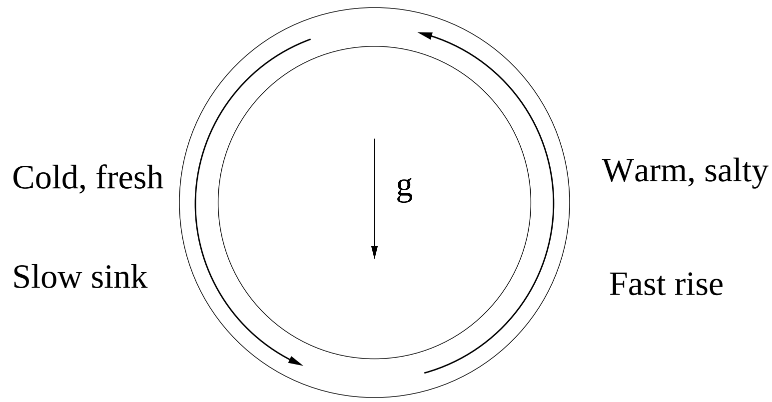

Figure 6: *Sketch of the oscillation mechanism.*

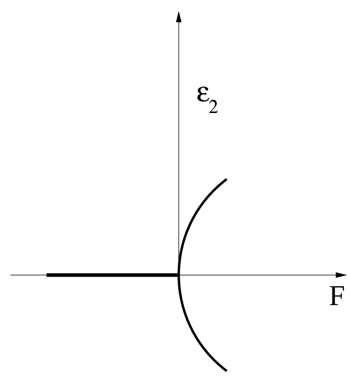

Figure 7: *Schematic plot of a Hopf bifurcation*

The effect of noise

Suppose now that the salinity flux consists of an average part $\bar{F}$ and a random part $F'(t)$, where the noise has variance $< F'^2 > dt = \sigma^2$. This noise can excite oscillations even when $\bar{F} < 0$, that is when the associated deterministic system has a stable fixed point. We compute again steady states and perform linear stability analysis to get

$$\ddot{\epsilon}_2 + \epsilon_2 - \bar{F}\dot{\epsilon}_2 = F'.$$

We can solve the system using Fourier Transforms, so

$$-(\omega^2 - i\omega\bar{F} - 1)\tilde{\epsilon}_2 = \tilde{F}'.$$

Then the spectrum is

$$< |\tilde{\epsilon}_2|^2 >= \frac{< |\tilde{F}'|^2 >}{(\omega^2-1)^2 + \omega^2\bar{F}^2} = \frac{\sigma^2}{dt[(\omega^2-1)^2 + \omega^2\bar{F}^2]}. \tag{39}$$

A typical spectrum is plotted in Fig. 8. Characteristic of the spectrum of such a system is that it peaks at the intrinsic frequency, which is $\omega = 1$ in this case, and that the height depends on the noise variance.

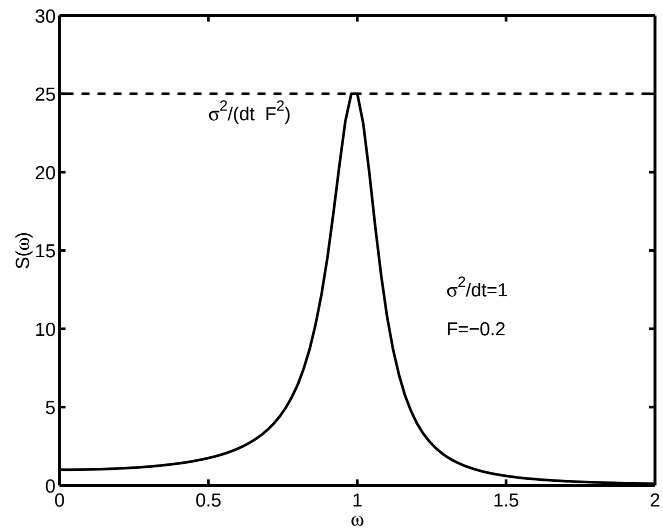

Figure 8: *A typical example of the spectrum of equation 39. Values that were used were* $f = -0.2$ *and* $\sigma^2/dt = 1$. *The height of the spectrum is* $\sigma^2/(dtF^2)$.

7 Welander's flip-flop oscillation

Another conceptual model of the thermohaline circulation is the so-called flip-flop model of Welander. It consists of a box of temperature T and salinity S that can exchange heat and salt vertically with a reservoir that is kept at temperature T_0 and salinity S_0 (see Fig 9).

The surface box is relaxed towards a temperature T_A and is forced by a freshwater flux

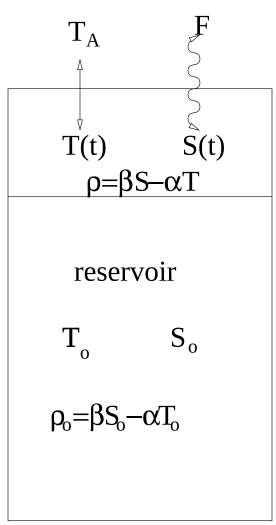

Figure 9: *Welander's flip-flop model*

F. Again, a linear equation of state is used for both boxes, so that $\rho = \beta S - \alpha T$ for the upper box and $\rho_0 = \beta S_0 - \alpha T_0$ for the reservoir. The equations that describe the evolution of temperature and salinity in the upper box are given by

$$\begin{aligned}
\dot{T} &= -\gamma(T - T_A) - \kappa(T - T_o), \\
\dot{S} &= F - \kappa(S - S_o).
\end{aligned} \tag{40}$$

where γ is a relaxation coefficient, κ a mixing coefficient that is taken equal for heat and salt and H is the thickness of the upper box. The mixing coefficient is taken to be dependent on the density difference between the two boxes, to represent the effect of convection. Mixing with the reservoir is much faster if the stratification is unstable than if it is stable:

$$\kappa = \begin{cases} \kappa_1 & \text{if } \rho - \rho_o \leq \Delta\rho \\ \kappa_2 & \text{if } \rho - \rho_o > \Delta\rho. \end{cases}$$

with $\kappa_2 \gg \kappa_1$. Introducing new variables

$$x \equiv \frac{T - T_o}{T_A - T_o}, \; y \equiv \frac{\beta(S - S_o)}{\alpha(T_A - T_o)}, \; t' \equiv \gamma t,$$

we can rewrite 40 to

$$\begin{aligned}
\dot{x} &= 1 - x - \nu x \\
\dot{y} &= \mu - \nu y.
\end{aligned}$$

Here we have definex $\mu = \beta F/(\gamma\alpha H(T_A - T_0))$ and

$$\nu = \frac{\kappa}{\gamma} = \begin{cases} \nu_1 & \text{if } y - x \leq \epsilon \\ \nu_2 & \text{if } y - x > \epsilon, \end{cases}$$

with $\epsilon = \Delta\rho/(\alpha(T_A - T_0)$.

The steady states of the model are

$$x = \frac{1}{1 + \nu}, \quad y = \frac{\mu}{\nu}.$$

Thus there are steady states if the density satisfies

$$\begin{aligned}
\text{either } y - x &= \frac{\mu}{\nu_1} - \frac{1}{1 + \nu_1} \leq \epsilon \\
\text{or } y - x &= \frac{\mu}{\nu_2} - \frac{1}{1 + \nu_2} > \epsilon.
\end{aligned}$$

In the first case, the stratification is stable and 'convection' never occurs, in the latter case the stratification is unstable and there will always be 'convection'. No steady states can *exist* if

$$\mu_1 < \mu < \mu_2$$

with

$$\mu_2 \equiv \epsilon\nu_2 + \frac{\nu_2}{1 + \nu_2}, \quad \mu_1 \equiv \epsilon\nu_1 + \frac{\nu_1}{1 + \nu_1}$$

For $\mu_1 < \mu < \mu_2$ the fixed point *disappears* and the system has relaxation-oscillations (Fig. 10). The system follows a slow relaxation towards the unstable, always convecting

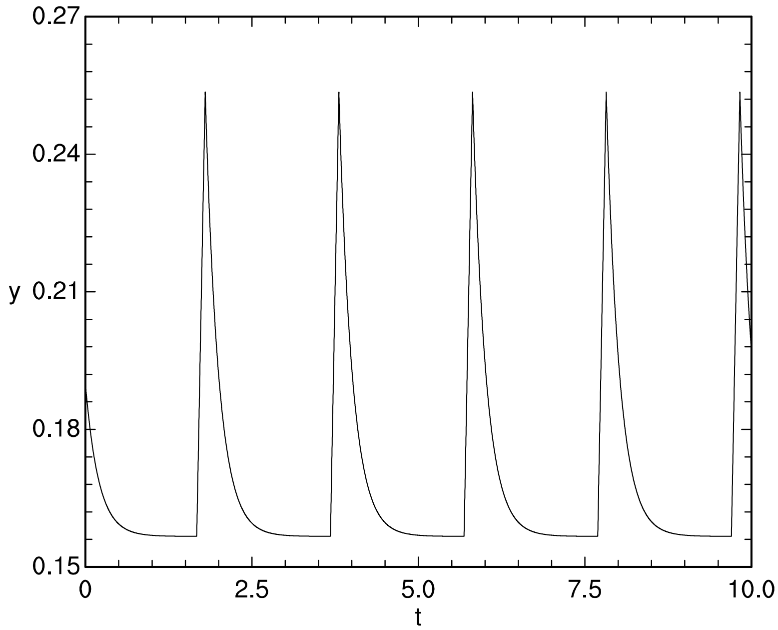

Figure 10: *Relaxation oscillations for Welander's flip-flop model.*

state, but before the steady state is actually reached the stratification becomes stable due to the strong mixing in the convecting state. As soon as a stable stratification is reached, the mixing coefficient becomes small (ν_1) and convection stops. Now the surface freshwater flux starts to increase the salinity of the upper box [this corresponds to $y \equiv \beta(S - S_0)/(\alpha(T_A - T_0))$ becoming larger], so that the density of the upper box increases strongly and the system evolves towards the stable, never-convecting state. However, before this equilibrium is reached, the stratification becomes unstable and convection will start again. The amplitude of this type of oscillations is finite and the period τ is given by

$$\tau = -\frac{\ln \delta}{\nu_2}.$$

where $\delta = \mu_2 - \mu$ and $0 < \delta \ll 1$. The period of the oscillation thus depends on the distance from the critical parameter (in this case μ_2). Note that type of oscillations differ fundamentally from the oscillations in the Howard-Malkus-Welander loop that arose as the system went through a Hopf bifurcation. Now the steady state does not become unstable, it simply ceases to exist. Another difference with the Hopf bifurcations is that there are no damped oscillations for $\mu > \mu_2 + \delta$, whereas damped oscillations exist in the case of the Hopf bifurcation.

The effect of noise

To study the effect of noise we suppose again that the salinity flux consists of an average part that is now called $\bar{\mu}$ and a random part $\mu'(t)$, where the noise has variance $< \mu'^2 > dt = \sigma^2$. This noise excites oscillations in the fixed point regimes, $\bar{\mu} < \mu_1$ and $\bar{\mu} > \mu_2$ (see Fig. 11). If there is no noise, the system goed to a stable, always convecting state (see the dashed line in Fig. 11). If noise is added to the system, there will be fluctuations that make the fluid in the upper box light enough to give a stable stratification so that convection stops. At this moment the system goes towards the other equilibrium.

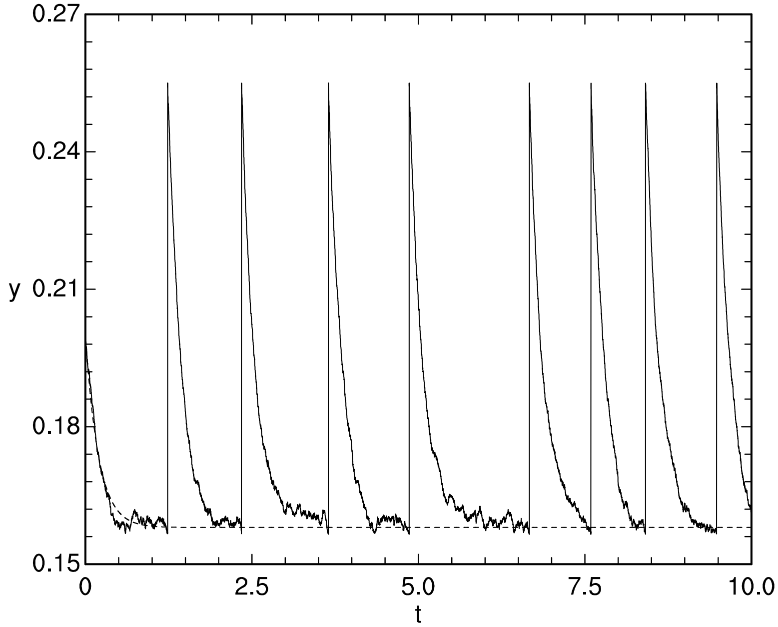

Figure 11: *The solid line gives the relaxation oscillations for Welander's flip-flop model in the stable regime $\bar{\mu} > \mu_2$ in the case with noise. The dashed line gives the solution for the same parameter values, but without noise.*

To make the computations easier, we now replace the fast relaxation to the convecting state with an instantaneous adjustment, so that the equations for the system with noise become

$$\begin{aligned} \dot{y} = \bar{\mu} + \mu' - \nu_2 y \quad &\text{if} \quad y \geq \mu_2/\nu_2 \\ y \to y_{max} \quad &\text{if} \quad y < \mu_2/\nu_2. \end{aligned}$$

where y_{max} is the value of y after the adjustment to the convecting state. Define now $\phi(y,t)dy$ as the probability that a certain realization of this experiment gives a salinity gradient between y and $y+dy$ at time t, so that $\phi(y)$ is again the probability distribution function (PDF). The average frequency of pulses is the probability flux $J(y_{max})$ through the point y_{max}. The PDF is governed by the Fokker-Planck equation (Gardiner, 1985):

$$\phi_t = J_y, \qquad J = (\nu_2 y - \bar{\mu})\phi + \sigma^2 \phi_y/2,$$

with boundary conditions

$$\phi(y < \frac{\mu_2}{\nu_2}) = 0$$

and

$$J(y = \frac{\mu_2}{\nu_2}, t) = J(y_{max}, t)$$

The first boundary condition says that y cannot take values under μ_2/ν_2, because as soon as $y < \mu_2/\nu_2$ we have $y \to y_{max}$. The second condition states the adjustment rule, which in turn corresponds to requiring that any member of the ensamble that goes through the threshold μ_2/ν_2 reappears with a value y_{max}. This is equivalent to say that the flux of states for these two values must coincide.

We can solve the steady Fokker-Planck equation using the normalization condition

$$\int_{\frac{\mu_2}{\nu_2}}^{y_{max}} dy\, \phi(y) = 1.$$

For weak noise and $\mu \approx \mu_2$ we obtain (Cessi, 1996)

$$J(y_{max}) \approx -\nu_2 \ln \frac{\sigma}{\sqrt{\nu_2}},$$

The average frequency of pulses is given by $\omega_{av} = 2\pi J(y_{max})$, and so this depends on $\sigma/\sqrt{\nu_2}$, which is the noise amplitude. The spectrum peaks at a frequency that depends on σ, but the height is independent of σ.

8 Summary

Both in the Howard-Malkus-Welander loop and in Welander's flip-flop model oscillations can be found that are either self-sustained, or that can be excited by noise. However, the characteristics of these two types of oscillations are quite different. Self-sustained oscillations in the Howard-Malkus-Welander loop occur through a Hopf bifurcation, the amplitude is proportional to the distance between the parameter and the critical value of that parameter and the period is finite.

The oscillations in Welander's flip-flop model instead occur because the steady state ceases to exist (global bifurcation). The oscillation arising through this global bifurcation are characterized by a finite amplitude even at onset and a period which depends logarithmically on the distance to the critical parameter value. Noise-induced oscillations in the Howard-Malkus-Welander loop have an amplitude that is proportional to the variance and a finite period, while noise-induced oscillations in the flip-flop model have finite amplitude and a period that depends logarithmically on the variance of the noise. This behavior is summarized in Table 1.

Notes by Taka Ito and Lianke te Raa

References

Cessi P., 1994: A simple box model of stochastically forced thermohaline flow. *J. Phys. Oceanogr.*, **2**, 1911-1920.

Cessi, P., 1996: Convective adjustment and thermohaline excitability. *J. Phys. Oceanogr.*, **26**, 481-491.

Self-sustained oscillations		
Dynamical behavior	Hopf bifurcation	Global bifurcation
Amplitude	$\propto \sqrt{\delta}$	finite
Period	finite	$\propto \ln \delta$
Example	HMW loop	Flip-flop model
Noise-induced oscillations		
Amplitude	$\propto \sigma$	finite
Period	finite	$\propto \ln \sigma$

Table 1: *Characteristics of the oscillations in the Howard-Malkus-Welander loop and in Welander's flip-flop model*

Dewar, W.K. and R.X. Huang, 1995: Fluid flow in loops driven by freshwater and heat fluxes. *J. Fluid Mech.*, **297**, 153-191.

Gardiner, C. W., 1990: Handbook of stochastic methods for physics, chemistry, and the natural sciences, 2nd ed., Springer-Verlag.

Huang, R.X. and R.L. Chou, 1994: Parameter sensitivity study of the saline circulation. *Climate Dyn.*, **9**, 391-409.

Mikolajewicz, U. and E. Maier-Reimer, 1990: Internal secular variability in an ocean general circulation model. *Climate Dyn.*, **4**, 145-156.

Tritton, D. J., 1988: Physical fluid dynamics, 2nd ed., Oxford University Press, 1988.

Welander, P., 1982: A simple heat-salt oscillator. *Dyn. Atmos. Oceans*, **6**, 233-242.

Welander, P., 1986: Thermohaline effects in the ocean circulation and related simple models. In *Large-scale transport processes in oceans and atmosphere*, J. Willebrand and D.L.T. Anderson, Eds., NATO ASI Series, Reidel, 163-200.